

High temperature C/C–SiC composite by liquid silicon infiltration: a literature review

MANISH PATEL*, KUMAR SAURABH, V V BHANU PRASAD and J SUBRAHMANYAM

Defence Metallurgical Research Laboratory, Hyderabad 500 058, India

MS received 27 November 2007; revised 1 March 2011

Abstract. The ceramic matrix carbon fibre (CMC) reinforced composite has received great attention for use in aerospace engineering. In aerospace, the atmosphere is highly oxidative and experiences very high temperature. In addition to this, the materials require high thermal stability and high abrasion resistance in that atmosphere. The C/C–SiC composite meets with these requirements. In this paper, the C/C–SiC composite by liquid silicon infiltration is reviewed thoroughly.

Keywords. CMC; C/C–SiC composite; processing; properties; application.

1. Introduction

Materials are the base for the technology and advanced technology requires advanced materials, particularly in aerospace and military applications. Ceramic matrix composites is one such advanced material. Carbon fibre reinforced ceramic–matrix composites are gaining increasing attention because (i) the good oxidation resistance of the ceramic matrix makes the composites attractive for high-temperature applications and (ii) continuously decreasing price of carbon fibres makes the use of carbon fibre reinforced composites economically feasible. Carbon fibres have wide range of properties. The properties of carbon fibres depend upon organic fibre precursors (polyacrylonitrile (PAN), cellulose, pitch), processing conditions (carbonization and graphitization temperature) microstructure, shape and surface properties of fibres. They have low density which varies between 1749 and 2021 kg/m³. Carbon fibres exhibit a range of Young's modulus values between 50 GPa and 690 GPa and tensile strength values between 500 MPa and 4000 MPa. Based on the strength, modulus carbon fibres are classified into different categories. High modulus high strength fibres have Young's modulus of above 400 GPa and strength, 1700–2500 MPa. High modulus fibres have Young's modulus of 300–700 GPa and strength, 2000–2500 MPa. High strength fibres have Young's modulus of 200–250 GPa and strength above 2500 MPa. Low modulus and low strength fibres have only Young's modulus of 50–150 GPa and strength of about 500 MPa (Ermolenko *et al* 1990; Buckley and Edie 1993; Murdie *et al* 1993). The linear thermal expansion coefficient of carbon fibres varies between 2×10^{-6} and 4×10^{-6} . The electrical resistivity of carbon fibres varies between 0.4 to $70 \times$

$10^{-5} \Omega \cdot m$ for carbonized fibres and $0.003\text{--}0.6 \times 10^{-5} \Omega \cdot m$ for graphitized fibres (Ermolenko *et al* 1990). The high modulus fibres have higher thermal conductivity, higher density, and lower thermal expansion coefficient than low modulus fibres (Buckley and Edie 1993). Chemical stability of carbon fibres depends upon the initial organic fibre precursors and microstructure. However, excellent properties of carbon fibres cannot be utilized as fibre for structural application but these are used in the form of reinforcement in composite with different matrices (polymer, metal, ceramic and carbon).

In an inert atmosphere or vacuum, carbon–carbon composites retain their strength, modulus and other mechanical properties at high temperature. But they are limited in their industrial applications due to their high sensitivity to oxidative environments. C/C composites are oxidizable above 400–500°C, but a surface coating of ceramics can protect the matrix and fibres from oxygen attack (Wu and Wei 1993; Zhu *et al* 1998). Among the different refractive materials, SiC is the best choice for coating because SiC has high heat stability, superior strength at elevated temperatures and low density. Several processes have been developed for fabrication of C/C composites with addition of SiC. Processes include slurry infiltration and hot pressing, polymer conversion, liquid silicon infiltration and chemical vapour infiltration (Xu *et al* 1998). In a slurry infiltration process, ceramic slurry is infiltrated and requires high temperature sintering and pressing operation. Limitations of above process for SiC coating are mechanical, thermal and chemical damages of fibres due to high sintering temperatures and high applied pressure. It is less effective because of absence of viscous flow of SiC and also it is limited to only one or two dimensional reinforced composites. In the polymer conversion process, organosilicon polymer polycarbosilane is infiltrated and subsequent pyrolysis of the polymer is carried out at 1000°C for conversion to SiC. But the limitation of this process is due to high

*Author for correspondence (patelmet@yahoo.co.uk)

shrinkage and low SiC yields. Chemical vapour infiltration is a very well established process for uniform coating but is expensive and time consuming. The liquid silicon infiltration process, which was first developed at German aerospace Research Establishment, is less costly and quick to process. It consists of pyrolysis of carbon fibre reinforced plastic and subsequent liquid silicon infiltration of the C/C composite (Xu *et al* 1998). The oxidation resistance of C–C composite improves significantly by the silicon infiltration by forming SiC/C zone. C/C–SiC composites have low coefficient of thermal expansion, high thermal conductivity, moderate modulus and excellent thermal shock resistance. SiC imparts necessary resistance to abrasion (Krenkel 2003).

2. Processing

One major manufacturing process of the carbon fibre reinforced SiC composites materials is the liquid silicon infiltration (LSI) of a porous C/C preform to form C/C–SiC composite. The LSI process leads to a damage tolerant ceramic material that has a significantly lower component fabrication time and therefore, reduced component costs compared with other CMC manufacturing processes (Krenkel 2001). This process consists of three steps. (i) manufacturing of carbon fibre reinforced plastic (CFRP) preform by common methods like resin transfer moulding or autoclave technology. The bidirectionally reinforced

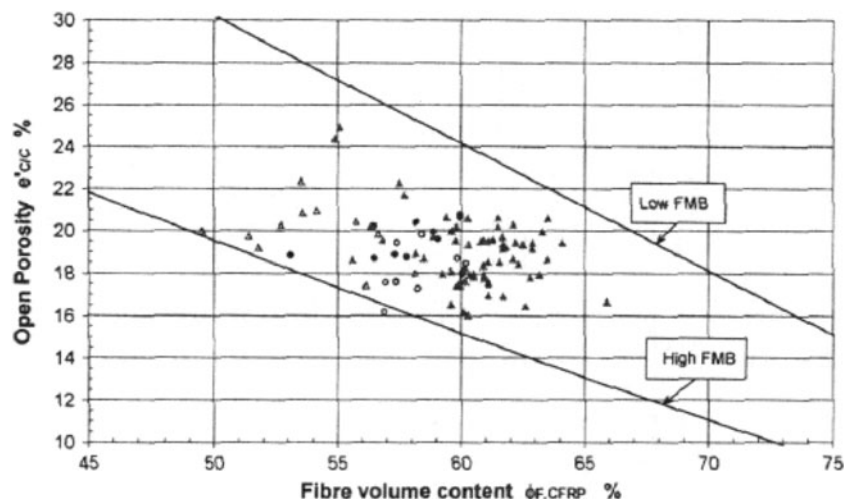


Figure 1. Variation of open porosity with fibre volume content of 2D-CFRP after pyrolysis (Krenkel 2001).

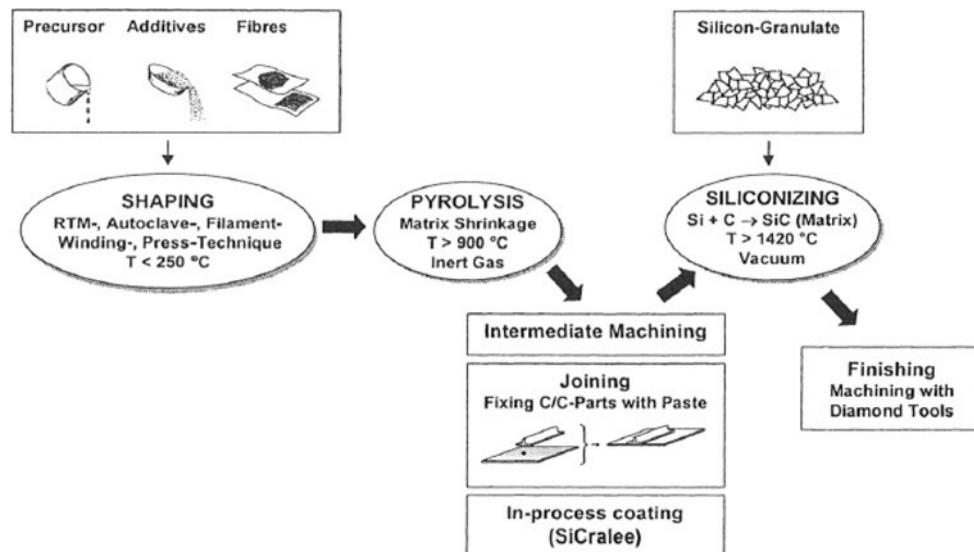


Figure 2. Process flow chart for production of C/C–SiC composite via liquid silicon infiltration process (Krenkel 2003).

CFRP with fibre contents of 60 volume % typically have the density of 1490 kg/m^3 and an open porosity of $<1\%$ (Krenkel 2001), (ii) conversion of the polymeric matrix into carbon by pyrolysis (900°C , inert atmosphere) thus forming a porous C/C preform. In this step, shrinkage of the polymeric matrix is hindered by the fibres which lead to the development of a regular crack pattern. After pyrolysis, the density is $\sim 1610 \text{ kg/m}^3$ and porosity increases. The variation in porosity after pyrolysis depends on the fibre volume content (figure 1) (Krenkel 2001) and (iii) the siliconization of C/C preform with liquid silicon results in reaction of carbon matrix with silicon and forms SiC. This yields a dense material with C/C segments separated from each other by SiC. After siliconization the density of the composites is around 2340 kg/m^3 , which is lower than the liquid silicon (2530 kg/m^3) (Krenkel 2001). In order to obtain successful siliconization, exact amount of silicon is required to ensure a complete filling of the C/C preform and avoid the danger of component destruction through excessive siliconization.

The complete process chart for liquid silicon infiltration process for a near net shape component is given in figure 2 (Krenkel 2003).

3. Microstructure

The microstructure of the C/C–SiC composites after different steps of processing depend upon the choice of matrix precursor and fibre structure, processing parameters and the fibre/matrix interface. Figure 3 shows the microstructure after pyrolysis (Schulte-Fischedick *et al* 2002). It contains the carbon fibres and carbon matrix. The carbon yield of the precursor is about 60 wt %. This leads to high shrinkage of the resin of about 20% in length (Schulte-Fischedick *et al*

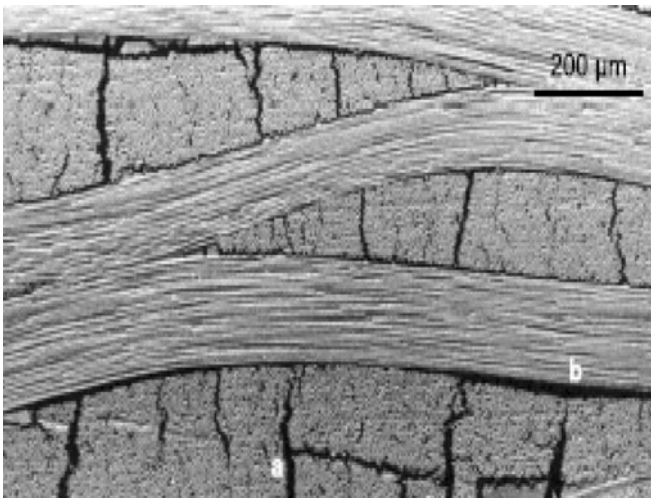


Figure 3. SEM micrograph of crack microstructure after pyrolysis at 900°C showing (a) segmentation cracks and (b) microdelaminations (Schulte-Fischedick *et al* 2002).

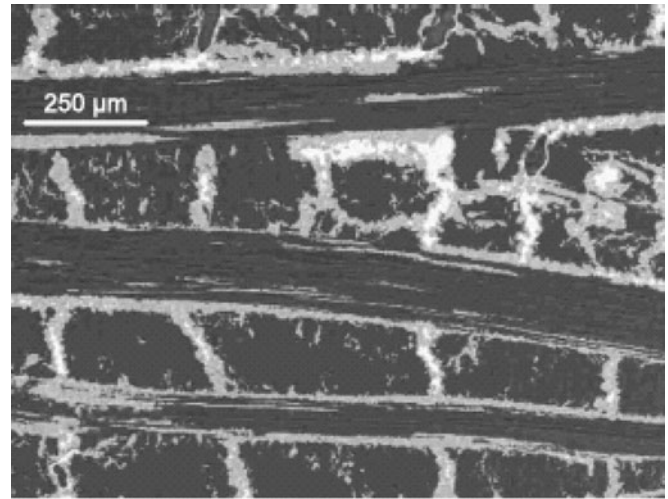


Figure 4. SEM micrograph presenting C/C–SiC with C/C segments (dark), SiC (grey) and silicon (white) (Schulte-Fischedick *et al* 2002).

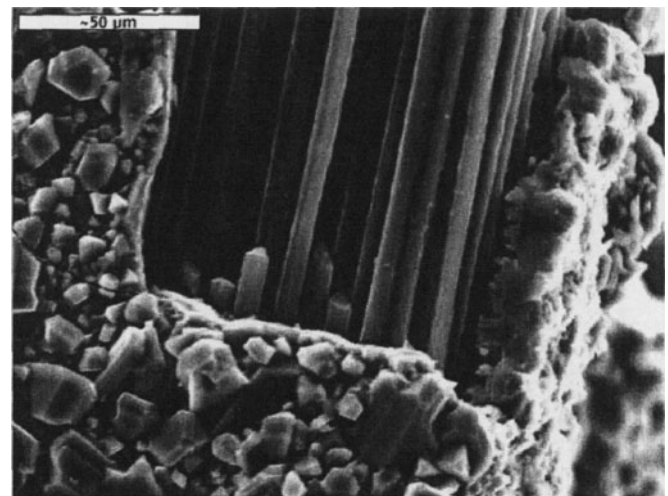


Figure 5. Layers of SiC of different crystal sizes around carbon fibres (Krenkel 2001).

2002). But the shrinkage in fibre direction is prevented by stiff fibres. This results in high amount of matrix cracking. Also there is fibre bundles segmentation in composites. This is due to a relatively higher coefficient of thermal expansion of carbon fibre transverse to the fibre axis, which creates transverse cracks as the matrix shrinkage is restrained parallel to the fibres. So the formation of the crack patterns depends on the fibre types, the weaving mode and the fibre/matrix bonding forces.

Siliconization results in a microstructure of C/C segments surrounded by SiC, in which unreacted silicon can be found. Figure 4 shows microstructure of the composite after siliconization (Schulte-Fischedick *et al* 2002). The micrograph shows dark region of C/C segments, grey region of SiC and

white region of unreacted silicon. Schulte-Fischedick *et al* (2002) and Krenkel (2001) have shown that the siliconized area consist of two types of SiC which can be distinguished by their crystal size. A fine grained SiC at the C/SiC interface is followed by a coarse grained SiC. Figure 5 shows different crystal sizes of SiC around carbon fibres (Krenkel 2001).

In the ideal case the infiltrated liquid silicon only reacts with the matrix carbon of the C/C preform, whereas the carbon fibres remain unchanged. But in most of the cases the carbon fibres get chemically attacked. Figure 6 shows the chemically attacked fibres (Muller *et al* 2001). To prevent carbon attack by the liquid silicon, there are two possibilities, either by coating or by suitable fibre arrangements (Krenkel 2001; Krenkel and Gern 1993). The above work has been

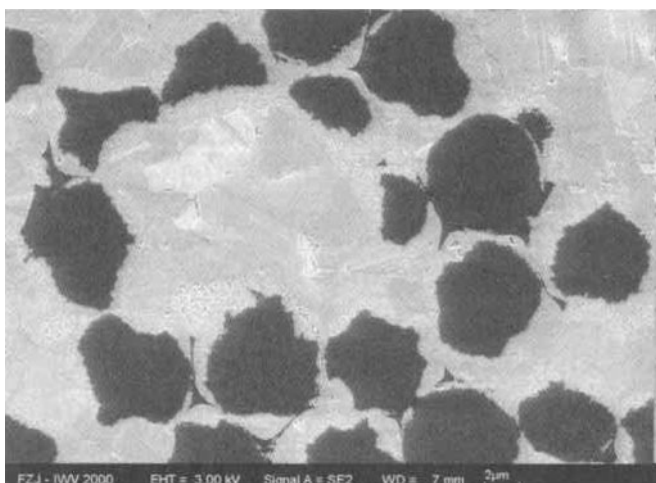


Figure 6. Micrograph showing reaction of carbon fibre with liquid silicon (Muller *et al* 2001).

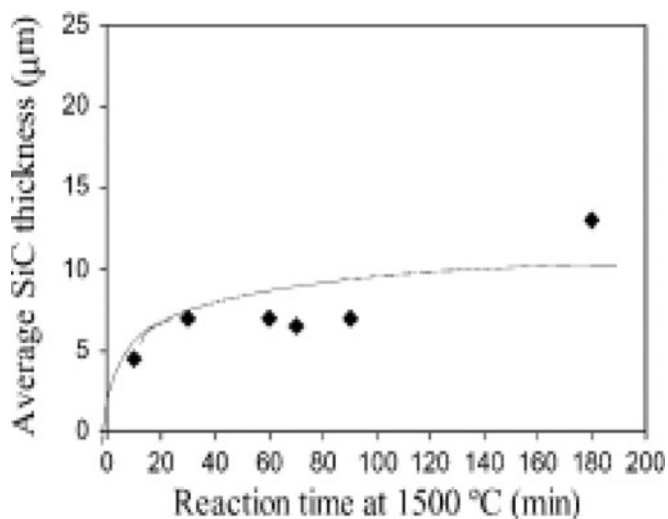


Figure 7. Thickness of SiC layer as a function of reaction time at 1500°C (Favre *et al* 2003).

focused on the development of controlled crack system with dense C/C regions of high fibre content and continuous channels between carbon fibres. The coating is expensive but still it is good for protection of fibres.

SiC, SiO₂, B₄C, TiC, Si₃N₄ and carbon are the possible coating materials for carbon fibres for protection from the chemical reaction of liquid silicon. Among ceramics mentioned above, SiC has excellent properties. The pyrolytic carbon layer coating is also useful for better properties because of the low interfacial bond energy. Generally, chemical vapour infiltration is used for coating which is a longer and expensive process. The thickness of pyrolytic carbon layer required depends upon the duration of siliconization because the thickness of SiC formation is time dependent. The average SiC thickness formed is plotted in figure 7 (Favre *et al* 2003). The above plot shows that the thickness of SiC layer remains nearly constant (about 10 μm) with time after around 45 min. Results are almost similar at 1500°C and 1600°C.

4. Mechanism of SiC formation during siliconization

In liquid silicon infiltration process, as silicon melts it goes into the preform and reacts with carbon and form SiC. There are two mechanisms for the formation of SiC by the reaction between carbon and silicon (Chiang *et al* 1991; Favre *et al* 2003).

(i) As the limiting step is the diffusion of carbon and silicon through SiC, this is a two-step mechanism. First step is the heterogeneous nucleation and growth of SiC which leads to the formation of a continuous polycrystalline SiC layer (Qian *et al* 2004). The initial layer is formed by the solid/gas reaction. As the silicon melts, silicon vapour and SiO (due to presence of very low quantity of oxygen) gas forms. A violent reaction occurs between the vapour and solid carbon and leads to nanocrystalline porous SiC with

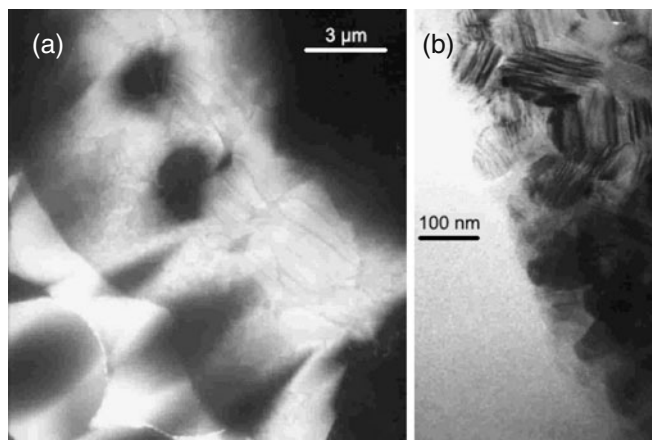


Figure 8. TEM images showing a nanocrystalline layer of SiC at interface C–SiC (Schulte-Fischedick *et al* 2002).

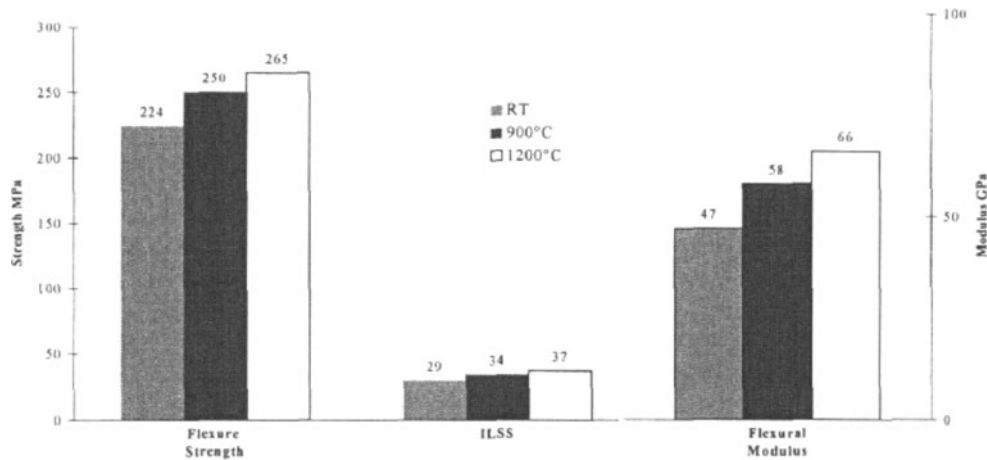


Figure 9. High temperature mechanical properties of C/C–SiC composites (Krenkel 2001).

high stacking faults. This reaction is away from the equilibrium. Second step is further growth of SiC. The growth of SiC is dependent on the diffusion of the reactive species (carbon and silicon) through porous SiC. There is contradiction about the growth of SiC by diffusion of carbon and silicon. Gern and Kochendorfer (1997) proposed a mechanism about the formation of SiC by assuming that the SiC formation is controlled by diffusion of silicon atoms through the SiC layer into the reaction zone. On the other hand, Hon and Davis (1979) and Hong and Davis (1980) have shown that the diffusion coefficient of carbon in SiC is 50–100 times higher than the diffusion of silicon through SiC. Hence the SiC layer growth proceeds by migration of carbon through SiC and consequent reaction at the SiC/Si interface. This contradiction can be explained by the microstructural observation of SiC layer near the carbon fibres. Schulte-Fischedick *et al* (2002) have shown through transmission electron microscopy that the nanocrystals are between C/C segments and larger grains (figure 8). Since the nanocrystal SiC formed, the reaction starts immediately and larger grains of SiC form after these nano layers. So this confirms the diffusion of carbon through the nanosized porous SiC.

(ii) Solution-precipitation mechanism: This second mechanism for formation of SiC is proposed by Pampuch *et al* (1986, 1987). In this mechanism, carbon is dissolved into liquid silicon followed by precipitation of SiC from the supersaturated liquid solution. The rate of formation of SiC by this mechanism is faster than the first mechanism. The exothermic dissolution of carbon in liquid silicon causes a local temperature rise at dissolution sites, which increases the solubility of carbon into melt. The carbon diffuses to local cooler sites where it precipitates as SiC.

As mentioned above, literatures conflict over these two mechanisms for formation of SiC. Microstructural characterization gives better evidence for the heterogeneous nucleation and growth of SiC by diffusion of carbon through porous SiC.

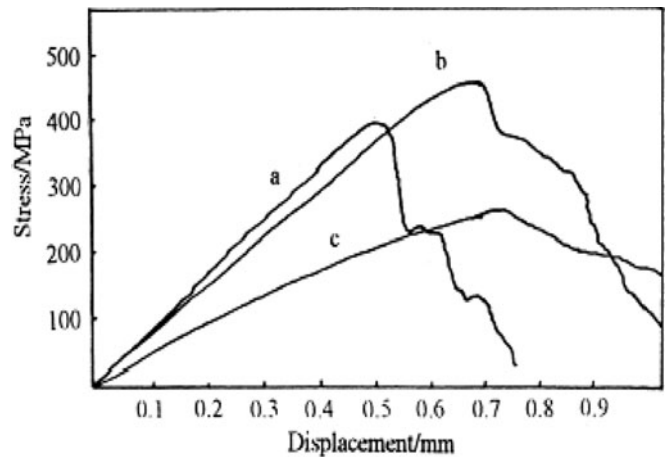


Figure 10. Stress–displacement curves for C/PyC/SiC composites with different interfacial layer thicknesses: a. 30 nm, b. 80 nm and c. 200 nm (Xu *et al* 1999).

5. Properties

5.1 Mechanical properties

C/C composites were developed to meet the needs of aerospace application that were resistant to high temperatures and were able to maintain structural integrity while experiencing the thermal stresses of reentry from space. For oxidation protection of C/C composites, C/C–SiC composites were developed by siliconization of C/C composites. So the mechanical properties of C/C–SiC composites depend upon the microstructure and temperature. Krenkel and Gern (1993) reported the tensile strength of C/C–SiC composite at room temperature with 55–65 vol % fibre content being around 90–115 MPa and elongation at break, 0.23%. The mechanical properties of C/C–SiC composites are given in figure 9 (Krenkel 2001). It shows that the mechanical

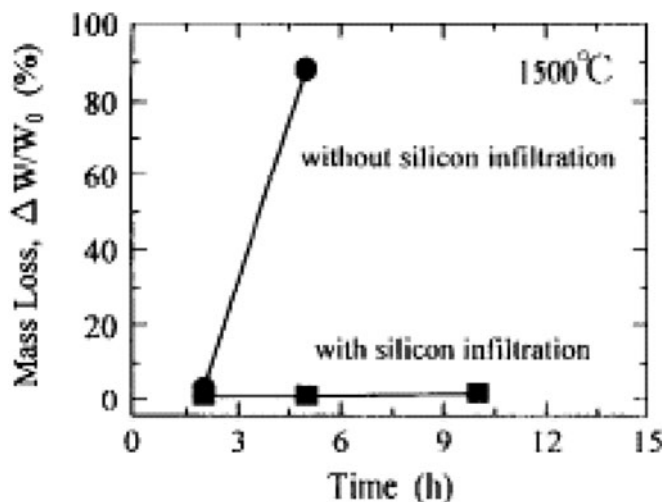


Figure 11. Effect of silicon infiltration on mass loss with time of CVD-SiC coated C/C composite (Zhu et al 1998).

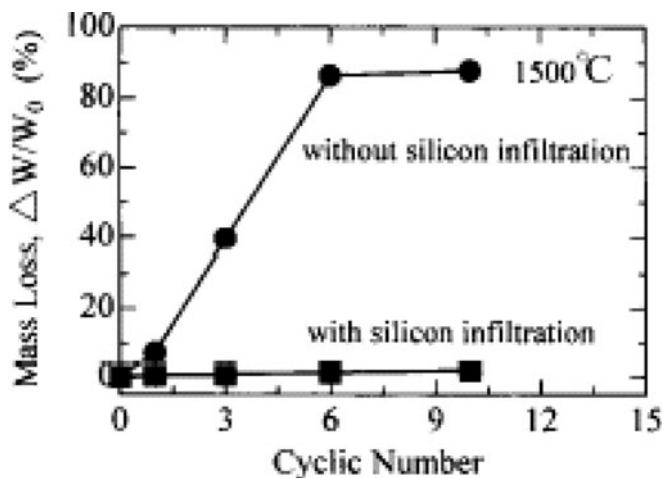


Figure 12. Effect of silicon infiltration on mass loss with cycle number of CVD-SiC coated C/C composite (Zhu et al 1998).

properties are better at higher temperature than at room temperature. Under stationary conditions (long term structural purpose), the maximum temperature range for C/C-SiC composites use is limited to 1500–1700°C. But one can use these composites up to 3000°C when the lifetime amounts to only a few min, like space or military application. Due to chemical attack of liquid silicon on carbon fibres the benefit of carbon fibre is not achieved. The room temperature compressive strength of this composite is around 300 MPa and shear strength is around 55–60 MPa. The interfacial layer of carbon in this composite has an important role to play in improving the mechanical properties because of the brittleness of both carbon fibres and SiC (Patel et al 2007). The interface is used to divert the crack and to reduce the matrix-fibre bonding. The thickness of the interface is also important because matrix-fibre bond strength decides

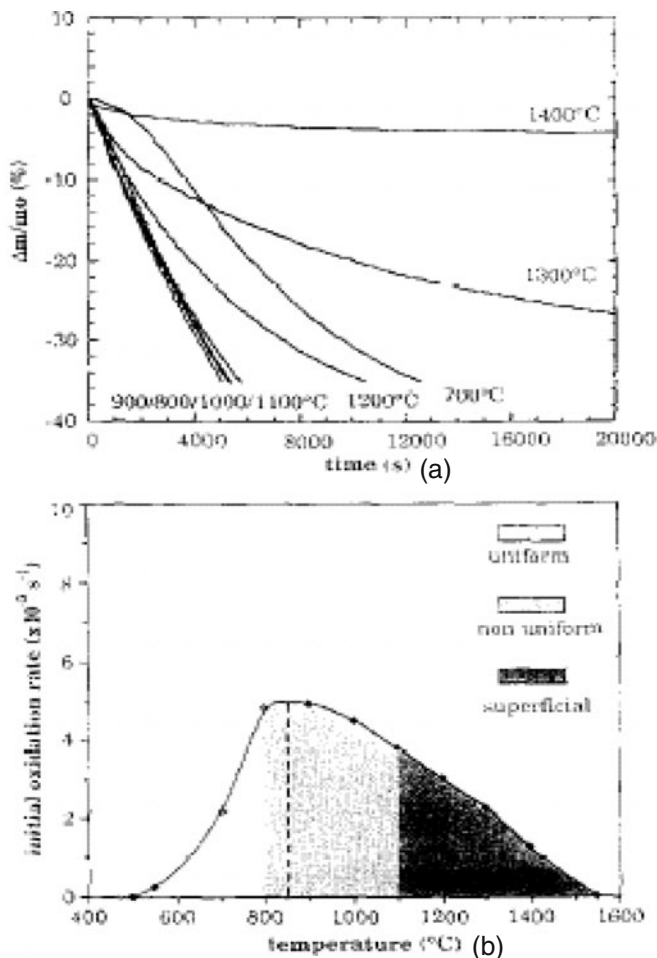


Figure 13. (a) Mass variations of C-C-SiC in oxygen as a function of time from TGA and (b) dependence of initial oxidation rate and mode of degradation of C-C-SiC composites to temperature of aging treatments performed under flowing oxygen (Lamouroux et al 1995).

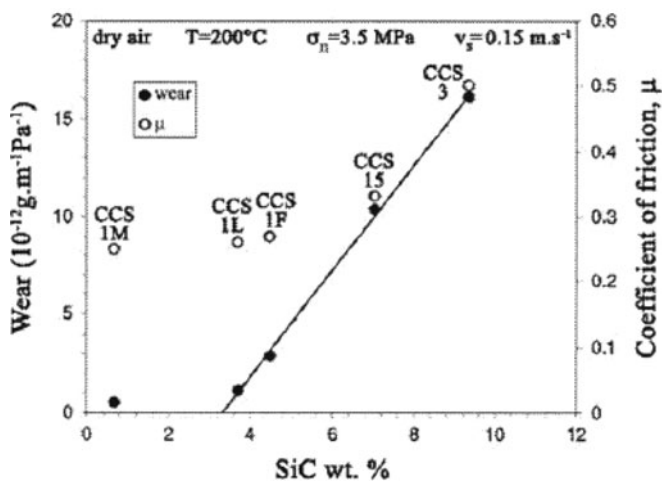


Figure 14. Variation of frictional properties of C/C-SiC composites with SiC content (Fillion et al 2005).

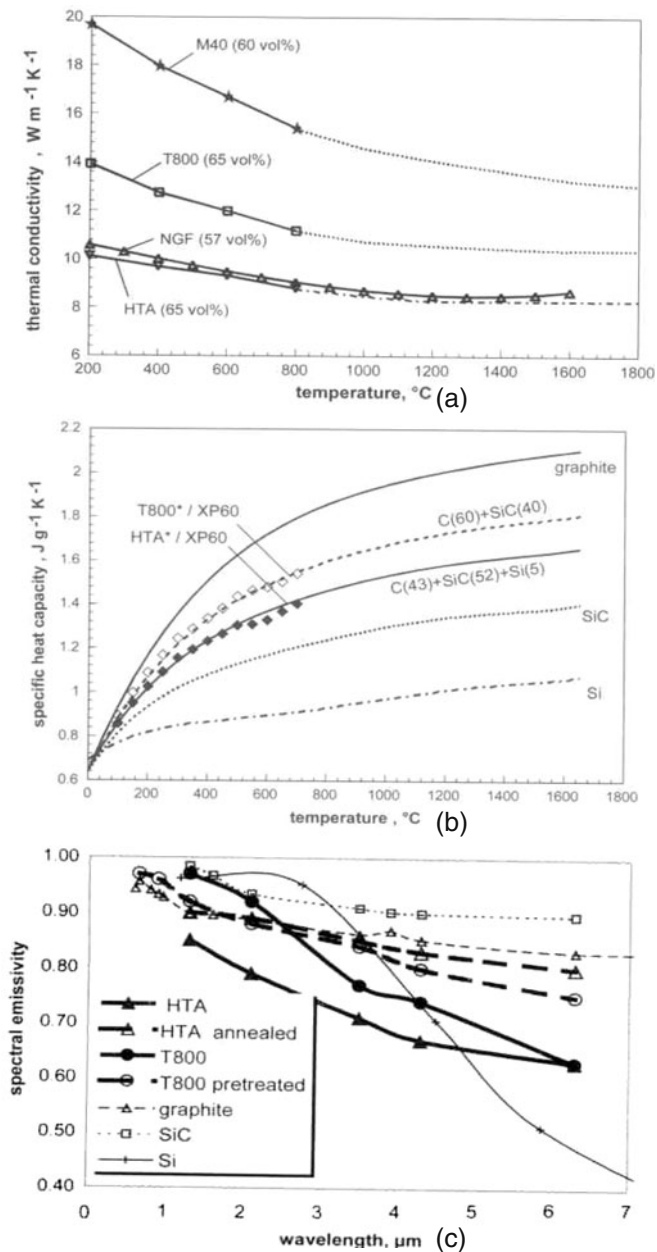


Figure 15. Variation of thermophysical properties: (a) thermal conductivity, (b) specific heat capacity and (c) spectral emissivity (Frieß *et al* 2001).

the mechanical properties of composites. The stress–displacement curve of C/SiC composite with carbon interface made by chemical vapour infiltration is given in figure 10 (Xu *et al* 1999). By increasing the thickness, the flexural strength increases and flexural modulus decreases.

5.2 Oxidation resistance

As C/C composites are exposed to an oxidizing environment at temperature >400°C, the carbon fibres react with oxygen and C/C composites lose their strength and damage

tolerance. So, successful application of C/C composite, therefore, requires a reliable protection to protect the carbon fibres from oxygen. SiC is a good oxygen barrier because it has excellent refractory properties. SiC is formed in C/C composite by liquid silicon infiltration. Figures 11 and 12 (Zhu *et al* 1998) show that the mass loss is very low for silicon infiltrated C/C composite as compared to that without silicon infiltration with increasing time as well as the heating and cooling cycle numbers. Transverse cracks form and oxygen diffuses through these cracks in C/C composites coated with CVD SiC, due to the large CTE mismatch between SiC and C (Lamouroux *et al* 1995). With silicon infiltration, a SiC/C interfacial zone forms with inner carbon to outer SiC. This zone plays an important role in minimizing the CTE mismatch which prevents the formation of cracks and therefore, increase the oxidation resistance (Krenkel and Berndt 2005). Experimentally the oxidation kinetics of the C/C–SiC composites can be studied by isothermal thermogravimetric analysis (TGA). Figure 13 shows the mass variation of C/C–SiC composite in oxygen with 100 kPa pressure with time by TGA (Lamouroux *et al* 1995). At low temperature (<800°C), the mass loss increases with temperature. It shows that the carbon–oxygen reaction controls the oxidation rate of the C/C–SiC composites, therefore, there is uniform degradation of the composite. Consequent result of this is severe decrease in tensile strength due to fibre notch effect. At intermediate temperature (800–1100°C), the mass loss nearly remains unchanged with time and temperature. It shows the oxidation kinetics is controlled by oxygen diffusion through the matrix micro cracks and therefore, results into a non-uniform degradation and a rapid decrease in tensile strength. At higher temperatures, >1000°C, the rate of mass loss decreases with time and temperature. It

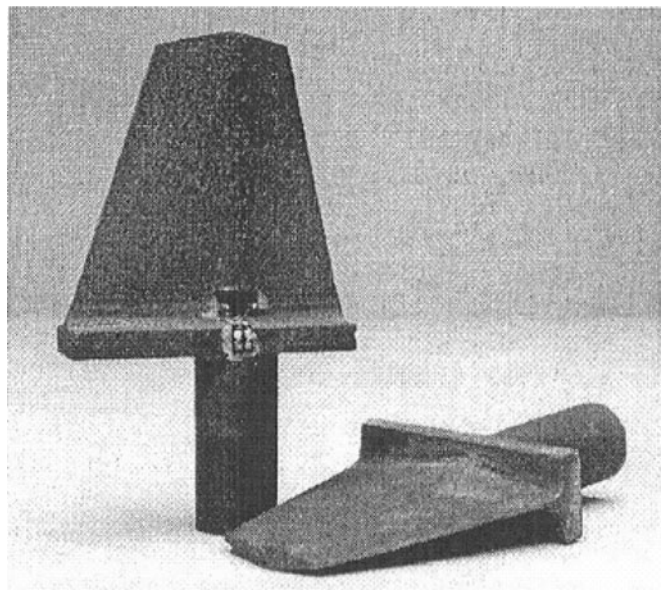


Figure 16. Jet vanes of C/C–SiC composites for missile or rocket (Krenkel 2003).

shows non constant oxygen diffusion mechanism, the oxidation takes place equally on the fibres and carbon interphase. So the oxidation rate is very high.

5.3 Wear resistance

Due to high thermal stability and low specific mass of C/C–SiC composites, it has great importance for advanced friction systems. The tribological properties of C/C–SiC composites are superior to C/C composites (Krenkel and Berndt 2005). For frictional application, C/C–SiC composites can be developed with a gradual increase of SiC from centre to the surfaces. But by increasing the SiC content and decreasing the carbon content influences the mechanical properties and decrease the damage tolerance of the brake disk. Also the SiC coating on the surface of C/C–SiC composite improves the wear resistance of the composites. Figure 14 shows the variation of friction properties of C/C–SiC composite with SiC contents in composite (Fillion *et al* 2005).

5.4 Thermophysical properties

The thermophysical properties of C/C–SiC composites are given in terms of thermal conductivity, specific heat

capacity, spectral emissivity and coefficient of thermal expansion. Krenkel and Gern (1993) reported the thermal conductivity of 2D–C/C–SiC composites in the range of 10–15 W/mK (parallel) and 6–8 W/mK (normal) for the temperature range of 200–1700°C. The specific heat capacity in the temperature range of 200–1700°C is 1150–1850 J/kgK. The total emissivity in the temperature range of 1000–1750°C is 0.65–0.75. The coefficient of thermal expansion in the temperature range of RT –1500°C is $1\text{--}2 \times 10^{-6}$ /K (parallel) and $4\text{--}6 \times 10^{-6}$ /K (normal). Frieß *et al* (2001) showed that the thermal conductivity and emissivity depend on carbon fibre tubes whereas the specific heat capacity is dependent on both the fibre and matrix properties. Figure 15 shows the variation of different thermophysical properties (Frieß *et al* 2001).

6. Applications

6.1 Jet vanes

Jet vanes are used to divert the direction of thrust in solid fuel rockets (figure 16) (Krenkel 2003). Here the operational time is very short, about a few seconds. At low speed phase, immediately after the rocket or missile takes off, the jet vanes provide control over the direction of rocket or

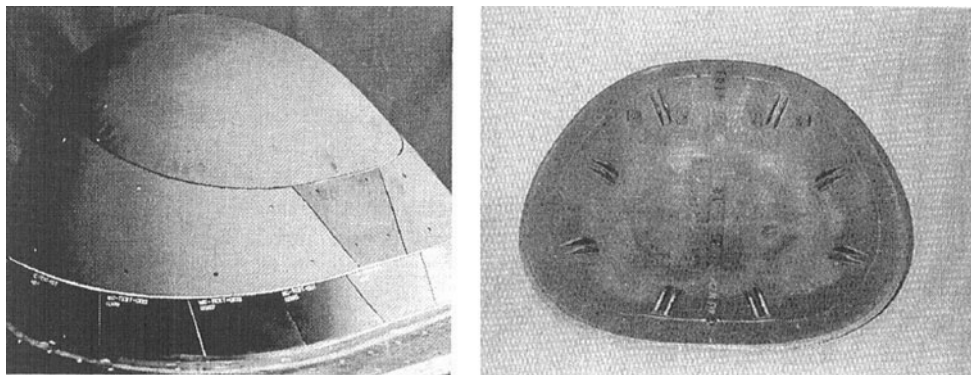


Figure 17. Nose cape of C/C–SiC composites for re-entry spacecraft (Krenkel 2003; Fischer 2004).

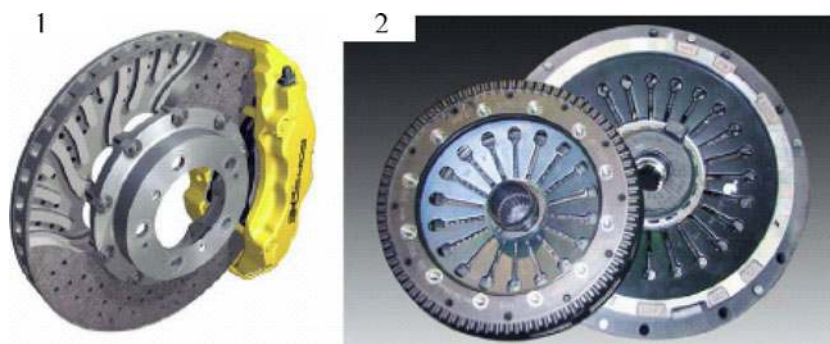


Figure 18. (1) Brake pads and (2) clutch of C/C–SiC composites (Krenkel 2005).

missile. In these few seconds, the material should perform with high thermomechanical stability and resistance to abrasion. These jet vanes are manufactured with C/C–SiC composites with two-dimensional fibre reinforcement. Due to their low coefficient of thermal expansion, high thermal conductivity and moderate strength, C/C–SiC composite shows excellent thermal shock stability. SiC imparts high resistance to abrasion.

6.2 Nose cap for re-entry spacecraft / aircraft brakes

During spacecraft re-entry into an oxidative atmosphere, the nose cap (figure 17) can reach surface temperatures up to 1800°C (Krenkel 2003; Fischer *et al* 2004). So, the materials involved demand a good wear resistance and high friction coefficients. C/C–SiC composites meet the above mentioned properties.

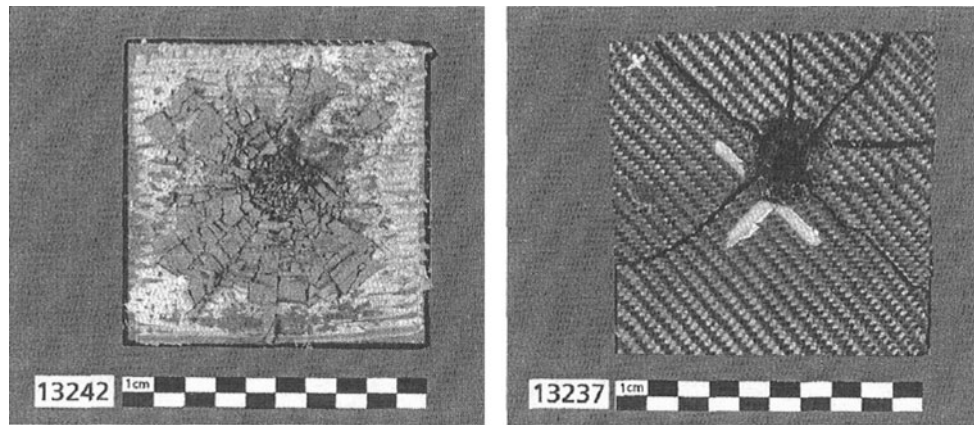


Figure 19. Light armor (1) biomorphous Si SiC and (2) C/C–SiC composite with Al backing after projectile impact with a speed of 850 m/s (Heidenreich *et al* 2003).

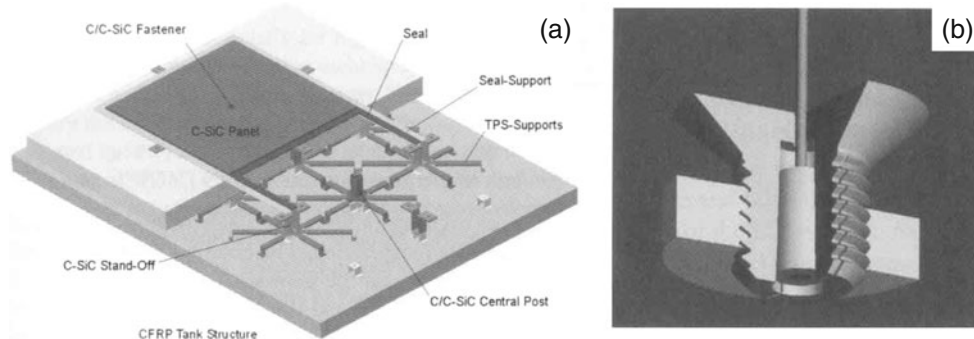


Figure 20. (a) Thermal protection systems and (b) threaded fastener of C/C–SiC composite (Kochendorfer *et al* 2001; Krenkel 2004).

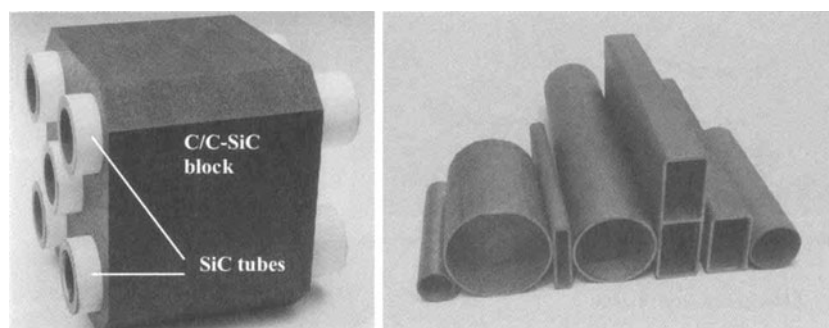


Figure 21. High temperature heat exchangers components of C/C–SiC composite (Kochendorfer *et al* 2001).

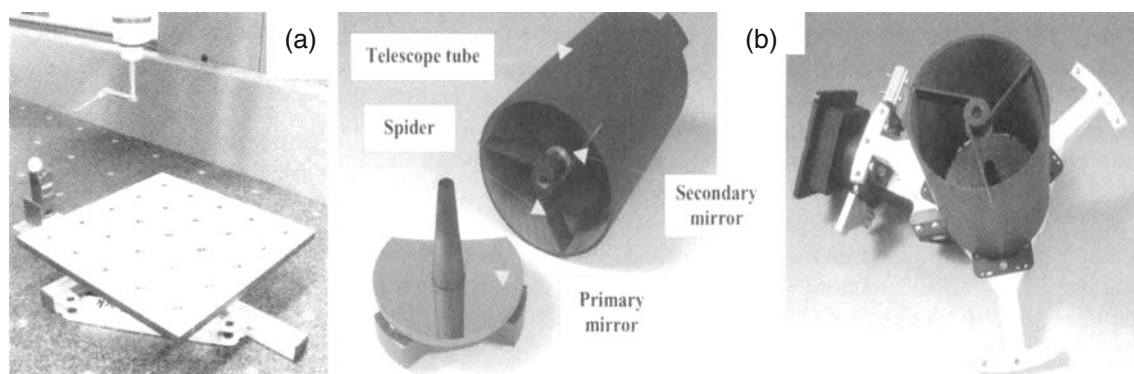


Figure 22. (a) Calibration ball plate and (b) telescope structure for data link between satellites of C/C–SiC composite (Kochendorfer *et al* 2001).

6.3 Brake pad

In combination with their low density, high thermal shock resistance and good abrasive resistance, they are promising candidates for advanced brake and clutch systems (figure 18) (Krenkel and Berndt 2005). High improvements in wear resistance were achieved by functionally graded C/C–SiC composites or by ceramic coatings. Almost wear-free brake disks in combination with acceptable low wear rates of the pads show a high potential for lifetime brake disks. Similarly, when an aircraft lands, the brakes can reach temperatures of up to 1000°C.

6.4 Light armor

The CMC armor (figure 19) (Heidenreich *et al* 2003) is very much lighter than the conventional armor. For ballistic protection, the required area weight of steel armor is three times higher than that of Al₂O₃/aramid armor system. But due to high brittleness and low fracture toughness, the monolithic ceramics armor does not show multiple hit capabilities. The fibre reinforced C/C–SiC composites show advantages concerning the multiple hit because the destroyed area is significantly smaller than monolithic ceramics (Heidenreich *et al* 2003). The biomorphic Si–SiC material shows the best result in single hit so it is possible to use both materials together and get best performance.

6.5 Thermal protection system (TPS) panel

TPS panel is one of the crucial elements for space application (Kochendorfer and Lutzenburger 2001; Krenkel *et al* 2004). It needs to have low mass and high temperature stability along with low coefficient of expansion. The C/C–SiC composites meet all these properties. Figure 20 shows the thermal protection system panel made of C/C–SiC composites.

6.6 Components for high temperature heat exchangers

Possible area for these composites is in the field of heat exchangers for high temperature processes like heat recovery

and heat waste recuperation. For this application materials need high strength, thermal shock resistance, gas tightness, good thermal conductivity and sufficient resistance for oxidation. The C/C–SiC composites have all these properties. Some of the components for the heat exchangers are given in figure 21 (Kochendorfer and Lutzenburger 2001).

6.7 Low temperature application

The flat plate shaped calibration bodies are used to determine length measurement irregularities to monitor coordinate measuring apparatus. For this application, materials need very low thermal expansion behaviour, high thermo-elastic stability, low density etc. The C/C–SiC composites fulfil the above criteria. Also, the optical system has high demand on precision and stability. Figure 22 shows some of the high precision components, which are made of C/C–SiC composites (Kochendorfer and Lutzenburger 2001).

Acknowledgements

Authors thank Director, Defence Metallurgical Research Laboratory, Hyderabad, for his continuous support and encouragement.

References

- Buckley D J and Edie D D 1993 *Carbon–carbon materials and composites* (USA: Noyes publications) pp 108–109
- Chiang M-Y, Messner P R, Terwilligner D C and Behrendt R D 1991 *Mater. Sci. Eng.* **A144** 63
- Ermolenko I N, Lyubliner P I and Gulko V N 1990 *Chemically modified carbon fibres and their application* (Germany: VCH) pp 6–7
- Favre A, Fuzellier H and Suptil J 2003 *Ceram. Int.* **29** 235
- Fillion A, Naslain R, Pailler R and Bourrat X 2005 *Ceram. Eng. Sci. Proc.* **26** 179
- Fischer I, Reimer T and Weihs H 2004 *Ceram. Eng. Sci. Proc.* **25** 275
- Frieß M, Krenkel W, Brandt R and Neuer G 2001 *Influence of process parameters on the thermophysical properties of C/C–SiC,*

- High temperature ceramic matrix composite* (eds) W Krenkel et al, pp 328–333
- Gern F H and Kochendorfer R 1997 *Composites Part A* **A28** 355
- Hon H M and Davis F R 1979 *J. Mater. Sci.* **14** 2411
- Hong D J and Davis F R 1980 *J. Am. Ceram. Soc.* **63** 546
- Heidenreich B, Krenkel W and Lexow B 2003 *Ceram. Eng. Sci. Proc.* **24** 375
- Kochendorfer R and Lutzenburger N 2001 *Application of CMCs made via the liquid silicon infiltration (LSI) technique, High temperature ceramic matrix composite* (eds) W Krenkel et al, pp 277–287
- Krenkel W 2001 *Ceram. Eng. Sci. Proc.* **22** 443
- Krenkel W 2003 *Ceram. Eng. Sci. Proc.* **24** 583
- Krenkel W and Gern F 1993 *Microstructure and characteristics of CMC manufactured via the liquid phase route, ICCM-9*, pp 173–181
- Krenkel W and Berndt F 2005 *Mater. Sci. Eng.* **A412** 177
- Krenkel W, Hausherr J M, Reimer T and Frieß M 2004 *Ceram. Eng. Sci. Proc.* **25** 49, 191
- Lamouroux F, Bourrat X and Naslain R 1995 *Carbon* **33** 525
- Muller M, Mentz J, Buchkremer P H and Stover D 2001 *Origin and effect of fibre attack for the processing of C/SiC, High temperature ceramic matrix composite* (eds) W Krenkel et al, pp 66–72
- Murdie N, Ju P C, Don J and Wright A M 1993 *Carbon–carbon matrix materials, carbon–carbon materials and composites* (eds) J D Buckley and D D Edie, pp 106–168
- Pampuch R, Walasek E and Bialoskorski J 1986 *Ceram. Int.* **12** 99
- Pampuch R, Bialoskorski J and Walasek E 1987 *Ceram. Int.* **13** 63
- Patel M, Saurabh K, Raju K S, Kumari S, Ghosal P, Bhanu Prasad V V and Subrahmanyam J 2007 *Preventing reaction of carbon fibres and liquid silicon during development of C/C–SiC composites, Proceeding of ICRACM*, pp 441–445
- Qian J, Jin Z and Wang X 2004 *Ceram. Int.* **30** 947
- Schulte-Fischedick J, Zern J, Mayer J, Ruhle M, Frieß M, Krenkel W and Kochendorfer R 2002 *Mater. Sci. Eng.* **A332** 146
- Wu T and Wei W 1993 *Mater. Chem. Phys.* **33** 208
- Xu Y, Zhang L, Cheng L and Yan D 1998 *Carbon* **36** 1051
- Xu Y, Cheng L and Zhang L 1999 *Carbon* **37** 1179
- Zhu Y, Ohtani S, Sato Y and Iwamoto N 1998 *Carbon* **36** 929